JVI Accepted Manuscript Posted Online 20 April 2016
J. Virol. doi:10.1128/JVI.00426-16

The SUMO Ligase Protein Inhibitor of Activated STAT 1 (PIAS1) is a constituent PML-NB protein that contributes to the intrinsic antiviral immune response to herpes simplex virus 1 (HSV-1).

James R. Brown[a], Kristen L. Conn[a], Peter Wasson[a,*1], Matthew Charman[a], Lily Tong[a], Kyle Grant[a*2], Steven McFarlane[a], and Chris Boutell[a,#]

MRC-University of Glasgow Centre for Virus Research (CVR), Sir Michael Stoker Building, Garscube Campus, Glasgow, Scotland, UK [a]

Running Head: PIAS1 is a PML-NB component intrinsic antiviral factor

Address correspondence to Chris Boutell, chris.boutell@glasgow.ac.uk

Present Address: MRC Technology, Edinburgh, Scotland, UK*[1], The Broad Institute, Cambridge Massachusetts, USA*[2]

K.L.C. and J.B. contributed equally to this work.

Word Count:

Abstract: 372

Text: 6167 (Introduction: 1049; M&M: 1759; Results: 2465; Discussion: 1438).

ABSTRACT

Aspects of intrinsic antiviral immunity are mediated by promyelocytic leukaemia (PML)-nuclear body (PML-NB) constituent proteins. During herpesvirus infection, these antiviral proteins are independently recruited to nuclear domains that contain infecting viral genomes to cooperatively promote viral genome silencing. Central to the execution of this particular antiviral response is the small ubiquitin-like modifier (SUMO) signalling pathway. However, the participating SUMOylation enzymes are not fully characterized. We identify the SUMO ligase Protein Inhibitor of Activated STAT1 (PIAS1) as a constituent PML-NB protein. We show that PIAS1 localizes at PML-NBs in a SUMO interaction motif (SIM)-dependent manner that requires SUMOylated or SUMOylation competent PML. Following infection with herpes simplex virus 1 (HSV-1), PIAS1 is recruited to nuclear sites associated with viral genome entry in a SIM-dependent manner, consistent with the SIM-dependent recruitment mechanisms of other well characterized PML-NB proteins. In contrast to Daxx and Sp100, however, the recruitment of PIAS1 is enhanced by PML. PIAS1 promotes the stable accumulation of SUMO1 at nuclear sites associated with HSV-1 genome entry, whereas the accumulation of other evaluated PML-NB proteins occurs independently of PIAS1. We show that PIAS1 cooperatively contributes to HSV-1 restriction through mechanisms that are additive to those of PML and cooperative with those of PIAS4. The antiviral mechanisms of PIAS1 are counteracted by ICP0, the HSV-1 SUMO-targeted ubiquitin ligase, which disrupts the recruitment of PIAS1 to nuclear domains that contain infecting HSV-1 genomes through mechanisms that do not directly result in PIAS1 degradation.

Importance. Adaptive, innate, and intrinsic immunity cooperatively and efficiently restrict the propagation of viral pathogens. Intrinsic immunity mediated by constitutively expressed cellular

proteins represents the first line of intracellular defence against infection. PML-NB constituent proteins mediate aspects of intrinsic immunity to restrict herpes simplex virus 1 (HSV-1), as well as other viruses. These proteins repress viral replication through mechanisms that rely on SUMO signalling. However, the participating SUMOylation enzymes are not known. We identify the SUMO ligase PIAS1 as a constituent PML-NB antiviral protein. This finding distinguishes a SUMO ligase that may mediate signalling events important in PML-NB-mediated intrinsic immunity. Moreover, this research complements the recent identification of PIAS4 as an intrinsic antiviral factor, supporting a role for PIAS proteins as both positive and negative regulators of host immunity to virus infection.

INTRODUCTION

Upon infection the host mounts a coordinated immune response that restricts the replication and pathogenesis of invading viral pathogens through the combined activities of intrinsic, innate, and adaptive immunity. A key distinguishing feature of intrinsic immunity is that it is mediated by constitutively expressed cellular restriction factors that act to limit the replication and spread of many viral pathogens [reviewed in (1-3)]. However, the mechanisms that regulate this aspect of host immunity remain to be fully elucidated.

Crucial to the intrinsic antiviral immune response during herpesvirus infection is the antiviral activity conferred by core constituent proteins associated with Promyelocytic leukaemia (PML) nuclear bodies (PML-NBs; also known as Nuclear Domain 10 [ND10]). Known restriction factors include PML (TRIpartite Motif 19; TRIM19), Sp100, Daxx, and ATRX, which influence the intracellular restriction of a diverse range of viruses (4). PML, the major

scaffolding protein of PML-NBs, is essential for PML-NB formation and coordinates a complex network of protein interactions dependent on sequences spanning its RBCC (RING, B-box, Coiled-Coil) tripartite motif (5). PML-NB formation is also heavily influenced by the post-translational modification of PML by Small Ubiquitin-like Modifier (SUMO) proteins (6-10), which promote non-covalent protein-protein interactions mediated by SUMO Interaction Motifs (SIMs) within individual PML-NB component proteins. Correspondingly, mutation of the RBCC motif, SUMO modification, or SIM consensus sequences within PML disrupts PML SUMO modification and the integrity of PML-NBs (9, 10).

SUMO modification regulates many cellular processes, including transcription, stress response, the cell cycle, and various aspects of host immunity to virus infection [reviewed in (2, 11)]. There are 3 major isoforms of SUMO (SUMO1-3) that are conjugated within mammalian cells. SUMO2 and SUMO3 share 97% amino acid identity (henceforth referred to as SUMO2/3) and can form poly-SUMO chains. SUMO1 shares ~50% amino acid identity with SUMO2, and is primarily associated with single SUMO modification or poly-SUMO chain termination events (12). Covalent attachment of SUMO to target substrates occurs in a sequential cascade analogous to that of ubiquitination, requiring E1 activating (SAE1/SAE2 heterodimer), E2 conjugating (Ubc9, also known as UBE2I), and E3 SUMO ligases [reviewed in (13-16)]. Whilst many SUMO modified substrates are directly conjugated by Ubc9, SUMO ligases enable the selective modification of substrates in response to a wide range of stimuli, influencing aspects relating to protein-protein interaction, stability, and sub-cellular localization. Viruses have therefore evolved strategies to exploit or inactivate the SUMO pathway during infection in order to promote their replication [reviewed in (2, 17, 18)].

During herpes simplex virus-1 (HSV-1) infection, SUMO modification plays a key role in the regulation of PML-NB mediated intrinsic antiviral immunity following viral genome entry into the nucleus. SUMO modification, SUMO-SIM interactions, and a functionally active SUMO pathway all contribute to the recruitment of PML-NB associated restriction factors to nuclear domains that contain infecting viral genomes (10, 19-21). Importantly, the recruitment of Sp100 and Daxx, as well as other SUMO2/3 conjugated proteins, to these domains occurs independently of PML (21, 22). The stable recruitment of constituent PML-NB antiviral factors correlates well with a cooperative restriction in viral gene expression (23, 24), a process that can limit the onset of productive infection and lead to the establishment of viral quiescence.

HSV-1 counteracts this aspect of host immunity through the expression of ICP0, a viral E3 ubiquitin ligase with SUMO-Targeted Ubiquitin Ligase (STUbL) properties. ICP0 induces the proteasome-dependent degradation or dispersal of PML-NB associated restrictions factors away from sites that contain infecting viral genomes [reviewed in (2, 25)], as well as broadly inducing the degradation of many other SUMO conjugated proteins (21, 26). ICP0 therefore inhibits the cellular restriction of viral gene expression and creates a favourable environment for the efficient onset of productive infection. Accordingly, ICP0-null mutant HSV-1, or HSV-1 mutants that express catalytically inactive ICP0, are more likely to enter into a non-productive quiescent infection at low multiplicities of infection (27-29). Importantly, the host-cell restriction of these viruses can be alleviated through the depletion of PML-NB associated restriction factors (22-24), inactivation of the SUMO pathway through the depletion of Ubc9 (21) or PIAS4 (30), or saturated upon increased multiplicity of infection (25). Taken together, these data highlight a key role for the SUMO pathway in coordinating PML-NB mediated

111 intrinsic antiviral immunity to HSV-1 infection. However, the SUMOylation enzymes that
112 mediate this aspect of host immunity remain to be fully defined.

113 We recently reported that the SUMO ligase Protein Inhibitor of Activated STAT 4
114 (PIAS4) contributes to the regulation of intrinsic antiviral immunity to HSV-1 infection in a
115 manner that is cooperative but independent of PML (30). Our identification of PIAS4 as an
116 intrinsic antiviral factor highlights a novel role for this family of proteins that have been
117 historically characterized as negative regulators of innate immunity [reviewed in (15, 16)]. As
118 PIAS proteins are known to regulate innate immunity through complementary but distinct
119 mechanisms, it is plausible that several PIAS proteins may also influence intrinsic antiviral
120 immunity to virus infection in a PML-NB dependent manner. Consistently, PIAS1 and PIAS2α
121 have been reported to localize to PML-NBs and to regulate PML SUMO modification (31). We
122 therefore investigated the potential roles of other PIAS family members in PML-NB mediated
123 intrinsic antiviral immunity.

124 We report that PIAS1 is the only family member to constitutively reside within PML-
125 NBs in uninfected human foreskin fibroblast cells in a PIAS1-SIM and PML SUMOylation-
126 dependent manner. During infection, PIAS1 was recruited to sites adjacent to HSV-1 genomes,
127 also in a PIAS1 SIM-dependent manner, where it colocalized with PML-NB constituent proteins
128 and other SUMO conjugated proteins. In contrast to Daxx and Sp100 (22), the efficient
129 recruitment of PIAS1 to these viral induced foci was enhanced by PML. To our knowledge this
130 represents the first example of a PML-NB constituent protein that is recruited in a largely PML
131 dependent manner. The stable recruitment of PIAS1 to these foci was disrupted by ICP0 without
132 inducing its proteasomal degradation, similar to ICP0 antagonism of Daxx (32). Depletion of
133 PIAS1, either alone or in combination with PML or PIAS4, increased the replication efficiency

of ICP0-null mutant HSV-1 but had no effect on the replication of a wild-type HSV-1. Taken together, our data demonstrate that PIAS1 and PIAS4 independently contribute towards the intrinsic antiviral immune response to HSV-1 infection as part of a coordinated host response to infection that is ultimately counteracted by the E3 ubiquitin ligase activity of ICP0.

MATERIALS AND METHODS

Cells, Drugs, and Viruses. HFt cells are immortalized human foreskin fibroblasts (HFs) (Department of Urology, University of Erlangen (22)) stably transduced with a vector that expresses the catalytic subunit of human telomerase, as described (33). HFt, HFs, and Retinal Pigmented Epithelial (RPE-1; ATCC, CRL-4000) cells were maintained in Dulbecco's Modified Eagle Medium (DMEM; Life Technologies, 41966). Human Embryonic Lung (HEL 299; ECACC, 87042207) fibroblast cells were maintained in Minimum Essential Medium Eagle (MEM; Sigma-Aldrich M5650) supplemented with 2 mM L-Glutamine (Life Technologies, 25030-024) and 1 mM Sodium Pyruvate (Life Technologies, 11360-039). HepaRG cells (34) were maintained in William's medium E (Life Technologies, 22551-022) supplemented with 2 mM L-Glutamine, 5 μg/ml insulin (Sigma-Aldrich, I2643), and 0.5 μM hydrocortisone (Sigma-Aldrich, H4881). Medium for all cell lines was supplemented with 10% foetal bovine serum (FBS; Life Technologies, 10270), 100 units/ml penicillin, and 100 μg/ml streptomycin (Life Technologies, 15140-122). Cells were maintained at 37^{o}C in 5% CO_2. HFt cells have an equivalent level of restriction of ICP0-null mutant HSV-1 replication as do HFs cells (data not shown).

MG132 (Calbiochem, 474790) prepared at 10 mM in DMSO (Sigma-Aldrich, D2650) was used at 10 µM. Doxycycline (DOX; Sigma-Aldrich, D9891) prepared at 1 mg/ml in Milli-Q H_2O was used at 0.1 µg/ml. For transgenic cells, Hygromycin (Invitrogen, 10687-010), Puromycin (Puro; Sigma-Aldrich, P8833), or Neomycin (Neo; Sigma-Aldrich, A1720) were used at 50 µg/ml, 1 µg/ml, or 1 mg/ml respectively, during selection, or 5 µg/ml, 0.5 µg/ml, 0.5 mg/ml respectively, for maintenance.

Wild-type HSV-1 strain 17*syn*+, ICP0-null mutant HSV-1 strain *dl*1403 (27), or their respective variants that express eYFP.ICP4 (35) were used. Viruses were grown and titrated as described (29). When used, MG132 was added 1 h after overlay of the inoculum. For infection of inducible transgenic cell lines, eYFP or eYFP fusion protein expression was induced with DOX for 4 h prior to infection in the absence of DOX. Infected cell monolayers were then overlaid with the appropriate media supplemented with DOX for the duration of the infection.

Plasmids and Lentiviral Transduction. An eYFP encoding sequence was PCR amplified and subcloned into the TOPO vector (Invitrogen) prior to insertion of the PIAS1 cDNA (Source Bioscience) between the EcoRI and KpnI restriction sites. The resultant eYFP.PIAS1 expression cassette was subcloned into the lentiviral vector pLKO.dCMV.TetO/R (36) using the NheI and SalI restriction sites. The primers used for PCR mutagenesis of PIAS1 and the resultant mutations are described in Table 1. All clones were confirmed by sequencing. Lentivirus vectors that express short hairpin (sh) RNAs against a non-targeted control sequence (shCtrl), PML (shPML) (22), PIAS4 (shPIAS4) (30), or PIAS1 (shPIAS1; based on: 5' TTGTAAGTCGTAAGGCATGGG 3') were obtained from the MISSION shRNA lentivirus vector collection (Sigma-Aldrich). Lentiviral supernatant stocks were produced and HFt cells

were transduced as described (22). Transgenic cells were pooled for experimentation. Transgenic HFt cells that expressed shRNA against PML were reconstituted with PML isoform I (PML.I) or a SUMOylation deficient PML isoform I (PML.I.4KR; substitution mutations at lysine residues 65, 160, 490 and 616) as described (10).

Antibodies. Primary rabbit: anti-actin (Sigma-Aldrich, A5060), anti-Daxx (Upstate, 07-471), anti-PIAS1 (LsBio, LS-B9173), anti-PIAS2 (LsBio, LS-C108717), anti-PIAS3 (LsBio, LS-C98795), anti-PIAS4 (LsBio, LS-C108719), anti-PML (Bethyl Laboratories, A301-167A), and anti-Sp100 (SpGH (37)). Primary mouse: anti-ICP0 (11060, (38)), anti-ICP4 (58S, (39)), anti-Daxx (AbD Serotec, MCA2143), anti-SUMO1 (Invitrogen, 33-2400), anti-SUMO2/3 (Abcam, ab81371), anti-UL42 (Z1F11 (40)), and anti-VP5 (DM165, (41)). Primary sheep: anti-SUMO1 (Enzo Life Sciences, BML-PW0505) and anti-SUMO2/3 (Enzo Life Sciences, BML-PW0510). Secondary antibodies: peroxidase conjugated anti-mouse IgG (Sigma-Aldrich, A4416), DyLight -680 or -800 conjugated goat anti-rabbit or -mouse IgG (Thermo), and Alexa-Fluor -488, -555, or -633 conjugated donkey anti-rabbit, -sheep or -mouse IgG (Invitrogen).

Immunofluorescence and Confocal Microscopy. HFt cells ($1x10^5$) seeded on 13-mm glass coverslips in 24-well plates were incubated at 37°C in 5% CO_2 overnight. For infections, virus was diluted in serum free DMEM to the multiplicity of infection (MOI) indicated in the corresponding figure legend. Inoculum was adsorbed for 1 h at 37°C in 5% CO_2 with rocking and rotating every 10 min, prior to overlay with 37°C cell appropriate media containing 2% Human Serum (HS; MP Biomedicals, 0929301). To examine the recruitment of host factors to nuclear sites associated with HSV-1 genome entry or replication compartments, cells were

typically infected at a low MOI for 16 h in order to visualize the distribution of host factors within newly infected cells at the periphery of a developing plaque edge (20). Fixation and immunostaining were performed at room temperature. Cells were washed twice in CSK buffer (10 mM Hepes, 100 mM NaCl, 300 mM Sucrose, 3 mM $MgCl_2$, 5 mM EGTA), fixed and permeablised in 1.8% formaldehyde (Sigma-Aldrich, F8775) and 0.5% Triton-X100 (Sigma-Aldrich, T-9284) in CSK for 10 min, then washed three times in CSK. Cells were blocked in 2% HS in PBS (Sigma-Aldrich, D1408) for 10 min, incubated with primary antibodies diluted in 2% HS in PBS for 90 min, then washed three times in PBS. DAPI (Sigma-Aldrich, D9542) and secondary antibodies diluted 1:1000 in 2% HS in PBS were added to the cells for 60 min, prior to three washes in PBS and two in Milli-Q H_2O. Coverslips were then mounted on glass slides with a glycerol-based mounting medium (Citifluor, AF1) and sealed with nail enamel. Samples were examined with a Zeiss LSM 710 confocal microscope with 405 nm, 488 nm, 543 nm, and 633 nm laser lines under a Plan-Apochromat oil immersion lens, numerical aperture 1.4. Zen 2012 software (Zeiss) was used to generate cut mask channels and weighted colocalization coefficients. Three dimensional image reconstruction was performed with Imaris (Bitplane) software. Images were minimally processed with Adobe Photoshop prior to assembly for publication with Adobe illustrator.

Western Blot. HFt cells (1.5 or 2.0 x 10^5) seeded in 12 well dishes were incubated overnight at 37°C with 5% CO_2, or for at least 4 h prior to further manipulation. For infection, 10 plaque forming units (PFU) per cell of wild-type or ICP0-null mutant HSV-1 were diluted in serum free DMEM. Inoculum was adsorbed for 1 h at 37°C in 5% CO_2 with rocking and rotating every 10 min, 37°C cell appropriate media was added, then cells were incubated at 37°C in 5% CO_2 until

harvest. Cells were washed twice with room temperature PBS and whole cell lysates were collected in SDS-PAGE loading buffer with 4 M Urea (Sigma-Aldrich, U0631) and 50 mM Dithiothretol (DTT, Sigma-Aldrich, D0632). Proteins resolved using standard Tris-glycine or Tris-tricine SDS-PAGE systems were electrotransferred onto 0.2 µm nitrocellulose membrane (Amersham, 15249794) at 250 mA for 150 (Tris-tricine) or 180 (Tris-glycine) min in Towbin buffer (25mM Tris, 192 mM glycine, 20% v/v methanol) at room temperature. Membranes were blocked in 5% FBS in PBS overnight at 4°C. Subsequent steps were performed on a roller apparatus at room temperature. Membranes incubated with primary antibody diluted in 5% FBS in PBS with 0.1% Tween (PBST; Calbiochem, 655204) for 2 h, were washed in PBST three times for 5 min each, then incubated with secondary antibody diluted 1:10,000 in 5% FBS in PBST for 1 h. Following three 5 min washes in PBST, one 5 min wash in PBS, and one rinse in Milli-Q H_2O, membranes were imaged on an Odyssey Infrared Imager (Licor). The intensity of protein bands was quantified using Odyssey Image Studio software.

Plaque Forming Efficiency (PFE). HFt cells (1×10^5) seeded in 24-well plates were incubated at 37°C in 5% CO_2 overnight. Wild type or ICP0-null mutant HSV-1 was serially diluted in serum free DMEM. Cells inoculated with sequential viral dilutions were rocked and rotated every 10 min for 1 h, then overlaid with 37°C cell appropriate media supplemented with 2% HS. Subsequent steps were performed at room temperature. 24 h post infection (hpi), cells were washed twice in PBS, fixed in 1.8% formaldehyde and 0.1% NP40 (BDH, 56009) in PBS for 10 min, then washed in PBST twice. Cells were blocked with 5% (w/v) skimmed milk powder (SMP; Marvel) in PBST for 30 min then incubated with anti-VP5 antibody diluted in 5% SMP in PBST for 90 min. Following three washes in PBST for 5 min each, peroxidase conjugated anti-

mouse IgG (Sigma-Aldrich, A4416) diluted in 5% SMP in PBST was added for 60 min. Cells were washed in PBST three times, then plaques were visualised using True Blue peroxidase developing solution (Insight, 50-78-02), according to the manufacturer's instructions.

Quantitative RT-PCR. 1.5 or 2.0 x 10^5 HFt cells seeded in 12-well plates were incubated at 37°C in 5% CO_2 overnight, or for at least 4 h before further manipulation. Cells were washed with PBS and total RNA was isolated using the RNAeasy Plus Kit (Qiagen, 74137) or Trizol reagent (Invitrogen, 15596) following the manufacturer's instructions. cDNA was synthesised using the TaqMan Reverse Transcription Reagents kit (Life Technologies, N8080234) with oligo (dT) primers. Samples were analysed in triplicate using TaqMan Fast Universal PCR Master Mix (Life Technologies, 4352042) with the following TaqMan gene specific primer-(FAM/MGB) probe mixes (Life Technologies): PML (Hs00231241_m1), PIAS1 (Hs00184008_m1), 18S (accession number X03205.1), or GAPDH (4333764F).

RESULTS

PIAS1 is a constituent PML-NB protein.

Although PML-NB-mediated restriction of viral replication is executed in part through SUMO-dependent processes (10, 21), the specific contributions of SUMOylation enzymes to this aspect of intrinsic immunity are not fully known. Using HFt human fibroblasts, which provide an amenable system to study PML-NB-mediated intrinsic immunity, we recently reported that the SUMO E3 ligase PIAS4 is an intrinsic antiviral factor. Even though PIAS4 is not a major PML-NB constituent protein in HFt cells (30), it is possible that several PIAS proteins confer intrinsic

antiviral activity and that some of which could regulate PML-NB-mediated viral restriction. To initiate investigation into the potential roles of PIAS proteins in PML-NB-mediated intrinsic immunity, whether any PIAS protein is a prominent constituent of PML-NBs in HFt cells was evaluated. PIAS proteins were predominantly nuclear in HFt cells and largely associated with matrix associated regions (MARs; Fig. 1A) (30). PIAS1 was the only family member that accumulated in punctate structures, which were identified to be PML-NBs by colocalization with PML (Fig. 1A) (30, 31). This localization of PIAS1 at PML-NBs was not unique to HFt cells and was evident in several other evaluated cell lines, including non-immortalized fibroblasts (HFs, HEL), hepatocytes (HepaRG), and epithelial cells (RPE) (Fig. 1C). The colocalization of PIAS1 with PML within HFt cells was nearly as prominent as that of Daxx, a major constituent protein of PML-NBs (Fig. 1) (42). The average weighted coefficient for colocalization of Daxx and PML was 0.89, whereas that of PIAS1 and PML was 0.65 (Fig. 1B). In contrast, PIAS2, PIAS3, and PIAS4 had minimal, if any, colocalization with PML (Fig. 1). These data identify PIAS1 as the only PIAS protein that substantially localizes to PML-NBs in HFt cells.

The localization of PIAS1 at PML-NBs is SIM-dependent and requires SUMOylated PML. SUMO-SIM interactions are vital for the localization of many constituent proteins at PML-NBs in uninfected cells (7, 8, 43). The role of SUMO-SIM interactions to mediate the steady state association of PIAS1 with PML-NBs was therefore evaluated. HFt cells were stably transduced with lentiviral vectors that could be induced to express eYFP or eYFP fused to wild-type PIAS1 or PIAS1 with point mutations in its SIM domain (Fig. 2A; Table 1). EYFP did not localize at PML-NBs (Fig 2B and D), nor did fusion to eYFP adversely affect PIAS1 localization at PML-NBs (Fig. 2C and E). Following short periods of induction PIAS1 colocalized with PML-NBs,

however, the sustained ectopic expression of PIAS1 (16 h) disrupted them (Fig. 2C) (30, 31). To avoid such adverse effects, catalytically inactive PIAS1 (eYFP.P1.C351A; Table 1) was subsequently used (44). Inactivation of the PIAS1 SUMO ligase activity did not abrogate PIAS1 localization at PML-NBs, nor did expression of this mutant disrupt PML-NBs (Fig. 2F, middle panel). Additional mutation of the SIM abrogated the localization of PIAS1 at PML-NBs (Fig. 2F, bottom panel), demonstrating that PIAS1 localizes to PML-NBs in a SIM-dependent manner that is largely independent of its SUMO-ligase activity.

The localization of PIAS1 at PML-NBs was evaluated in PML-depleted cells stably reconstituted with PML isoform I (eYFP.PML.I) or PML.I with substitution mutations in the four major SUMOylation acceptor sites (eYFP.PML.I.4KR) to test the potential dependency of PIAS1 localization at PML-NBs on PML SUMOylation (5, 10). PML depletion was achieved through the stable transduction of vectors that express PML specific short hairpin (sh) RNA (9, 22). The depletion of PML did not obviously affect PIAS1 expression (Fig. 3A). In the absence of PML, and consequently PML-NBs (7, 8), PIAS1 primarily localized to MARs (Fig. 3B). Reconstitution of PML depleted cells with eYFP did not stimulate the formation of PML-NBs or otherwise alter PIAS1 sub-nuclear localization (data not shown), whereas reconstitution with eYFP.PML.I was sufficient to nucleate PML-NB formation and PIAS1 associated with these structures (Fig. 3C). SUMO-modification of PML is essential for the proper assembly of PML-NBs (7, 8, 43), therefore, reconstitution with SUMOylation deficient PML.I resulted in the formation of aberrant aggregates (Fig. 3D) (8, 10). Some PML-NB constituent proteins, such as Daxx and SUMO1, associated with these aggregates while others, such as Sp100 and SUMO2/3, largely did not (Fig. 3D). The localization of Daxx at PML-NBs is largely mediated through SIM-dependent association with SUMO1, thus SUMO1 interaction with the PML.I.4KR SIM, or

317 the localization of an alternative SUMO1-modified protein at the PML.I.4KR aggregates, likely
318 mediated this association of Daxx (7, 43). In contrast, PIAS1 did not localize at the aggregates
319 of SUMOylation deficient PML. This data demonstrates that SUMO-modified, or SUMOylation
320 competent, PML is required for the stable association of PIAS1 at PML-NBs and that Daxx or
321 SUMO1 are not sufficient to mediate this association in the absence of SUMOylation competent
322 PML.
323
324 **The localization of PIAS1 at nuclear domains that contain infecting HSV-1 genomes is**
325 **disrupted by ICP0.**
326 ICP0 counteracts PML-NB-mediated intrinsic immunity by targeting specific antiviral proteins
327 for proteasome-dependent degradation or dispersal away from infecting viral genome foci
328 [reviewed in (25)]. Therefore, prior to investigation into the potential roles of PIAS1 in intrinsic
329 immunity, PIAS1 protein levels were evaluated during HSV-1 infection to ascertain whether it is
330 a substrate for ICP0-mediated degradation. HFt cells infected with wild-type HSV-1 had a
331 continued decrease in PIAS1 protein levels as infection progressed, down to 56 ± 9% of the
332 levels in mock-infected cells by 9 hours post infection (hpi; Fig. 4A and B; $P \leq 0.01$). In
333 contrast, PML, which is a direct target of ICP0, had a substantial loss (typically 50-70%) in
334 protein levels as early as 3 hpi (Fig. 4A). In the absence of ICP0, a significant loss in PIAS1
335 protein levels was not observed (Fig. 4A and B). Given the kinetics of PIAS1 degradation and
336 the lack of direct interaction with ICP0 (45), PIAS1 is not likely a substrate for ICP0-targetted
337 proteasomal degradation.
338 The relocalization of PML-NB constituent proteins from punctate PML-NBs throughout
339 the nucleus to a nuclear edge associated with HSV-1 genome entry is characteristic of the PML-

NB-mediated intrinsic immune response (for example see Fig. 4C PML, Daxx: ΔICP0) (10, 20). During ICP0-null mutant HSV-1 infection, PIAS1 also relocalized to the nuclear edge that contained infecting viral genomes, which was identified by the localization of PML or Daxx, and the HSV-1 DNA-binding protein ICP4 (Fig. 4C; ΔICP0). Reconstruction of a z-stack series of confocal microscopy images demonstrated that PIAS1 and PML colocalized at the nuclear edge associated with viral genome entry (Pearson coefficient 0.558), although foci that predominantly contained only PML or PIAS1 were also evident (Fig. 4D). The relocalization of PIAS1 to nuclear domains that contained infecting HSV-1 genomes was disrupted during wild-type HSV-1 infection (Fig. 4C; HSV-1). Under these infection conditions PIAS1 had a nuclear diffuse distribution similar to that of Daxx (Fig. 4C; HSV-1).

These data demonstrate that PIAS1 is recruited to nuclear domains that contain infecting HSV-1 genomes in a manner that is disrupted by ICP0 through mechanisms that do not directly target PIAS1 for degradation.

PML enhances PIAS1 SIM-dependent localization at nuclear domains that contain infecting HSV-1 genomes.

Constituent PML-NB antiviral proteins are individually recruited to nuclear domains that contain infecting HSV-1 genomes through SUMO-dependent mechanisms that are independent of PML (10, 20, 22). To initiate characterization of the recruitment mechanisms of PIAS1, its recruitment phenotype was evaluated in PML depleted cells. Robust depletion of PML was achieved through the stable transduction of plasmids that express PML specific shRNA (Figs. 3A, B and 5A) (22). As expected, Daxx was recruited to the nuclear edge associated with ICP0-null mutant HSV-1 genome entry independently of PML (Fig. 5A) (10, 22). In contrast, PIAS1

363 recruitment was significantly diminished in the absence of PML (Fig. 5A), suggesting that this
364 process is largely PML-dependent. PIAS1 was still stably recruited to nuclear domains that
365 contained infecting viral genomes in cells that expressed non-targeted control shRNAs,
366 confirming that the lack of recruitment was due to PML depletion and not transduction or the
367 selection of transgenic cells (Fig. 5A). These data demonstrate that PML promotes the stable
368 accumulation of PIAS1 in nuclear domains that contain infecting HSV-1 genomes.

369 Thus far, PIAS1 represents the first PML-NB constituent protein that is recruited to
370 domains that contain infecting HSV-1 genomes through mechanisms that are enhanced by PML.
371 As the association of PIAS1 with PML-NBs is SIM-dependent, the role of the SIM in the
372 recruitment mechanism of PIAS1 was evaluated. Mutation of the SIM substantially reduced
373 PIAS1 accumulation at the nuclear edge that contained infecting ICP0-null mutant HSV-1
374 genomes (Fig. 5B, ΔICP0 bottom panel). The reduced accumulation of mutant PIAS1 was not
375 due to the inactivation of its catalytic activity as the inactive PIAS1 mutant with a functional
376 SIM still stably accumulated in nuclear domains that contained infecting viral genomes (Fig. 5B,
377 ΔICP0 middle panel). As the expression levels of the mutant PIAS1 proteins were similar (Fig.
378 5C), the reduced accumulation of the SIM mutant was not due to overexpression saturating
379 potential binding sites within the nuclear domains that contained infecting viral genomes. As
380 expected, ICP0-mediated degradation of PML abrogated the recruitment of PIAS1 to the nuclear
381 periphery associated with infecting HSV-1 genomes regardless of any mutations to PIAS1 (Fig.
382 5B, HSV-1).

383 These data demonstrate that PIAS1 is recruited to nuclear domains that contain infecting
384 HSV-1 genomes through SIM-dependent mechanisms that are enhanced by PML. Furthermore,

385 the stable localization of PIAS1 at the nuclear edge associated with HSV-1 genome entry is
386 likely independent of PIAS1 catalytic activity.
387
388 **PIAS1 is not essential for PML SUMO modification or the formation of PML-NBs.**
389 The potential functional significance of PIAS1 to regulate the association of select PML-NB
390 constituent proteins at PML-NBs or their stable accumulation in nuclear domains that contain
391 infecting HSV-1 genomes was tested in PIAS1 depleted cells. Transgenic HFt cells that
392 expressed PIAS1 specific shRNA had a marked reduction in PIAS1 expression relative to cells
393 that expressed non-targeted control shRNA (Fig. 6A). After limited passaging, however, PIAS1
394 protein expression recovered to levels similar to those in transgenic cells that expressed control
395 shRNA (data not shown). Experiments were therefore conducted over multiple rounds of
396 independent transduction with minimal passaging of the isolated transgenic cells. The depletion
397 of PIAS1 did not noticeably alter PML expression or SUMO-modification (Fig. 6A) (31).
398 Furthermore, the association of the major constituent PML-NB proteins Daxx, SUMO1, or
399 SUMO2/3 at PML-NBs, or the relative size and number of PML-NBs per nuclei, were not
400 noticeably altered following PIAS1 depletion (Fig. 6B and C).
401 PML, Daxx, or SUMO2/3 still localized to sites associated with infecting ICP0-null
402 mutant HSV-1 genomes in PIAS1 depleted cells (Fig. 6D), demonstrating that PIAS1 is not
403 necessary for their stable accumulation in these domains. In contrast, the accumulation of
404 SUMO1 at the nuclear edge associated with viral genome entry was notably reduced in PIAS1
405 depleted cells (Fig. 6D), highlighting a role for PIAS1 in the stable accumulation of SUMO1 at
406 these sites. As expected, ICP0 efficiently disrupted the localization of constituent PML-NB

antiviral proteins at nuclear domains that contained infecting HSV-1 genomes regardless of the presence or absence of PIAS1 (data not shown).

These data demonstrate that PIAS1 is not essential for PML SUMOylation or the proper formation of PML-NBs. During ICP0-null mutant HSV-1 infection, PIAS1 is differentially required for the stable localization of constituent PML-NB proteins at nuclear domains that contain infecting viral genomes. The stable accumulation of SUMO1 at such domains is enhanced by PIAS1, whereas PML, SUMO2/3, or Daxx effectively re-localize to such domains independently of PIAS1.

PIAS1 contributes to the cellular restriction of ICP0-null mutant HSV-1.

To test the functional significance of PIAS1 during infection, the replication of wild-type or ICP0-null mutant HSV-1 was evaluated in cells depleted of PIAS1, or PML as a positive control (22). Transgenic HFt cells that expressed PIAS1 or PML specific shRNA, alone or in combination, had greater than 80% depletion in the specific target mRNA and a substantial reduction in the corresponding protein levels relative to cells that expressed non-targeted control shRNA (Fig. 7A and B). The depletion of PIAS1 did not substantially alter the plaque forming efficiency (PFE) of wild-type HSV-1, demonstrating that PIAS1 is not essential for HSV-1 replication (Fig. 7C). In contrast, the PFE of ICP0-null mutant HSV-1 was enhanced 10-fold in PIAS1 depleted cells, which was comparable to the increase observed following PML depletion (Fig. 7C). PIAS1 is thus identified as an intrinsic antiviral factor that contributes to the intracellular restriction of ICP0-null mutant HSV-1.

As the depletion of PIAS1 or PML resulted in a similar relief of restriction in ICP0-null mutant HSV-1 replication, and PML facilitates the stable accumulation of PIAS1 in domains that

contain infecting HSV-1 genomes, it is possible that the mechanisms of PIAS1 and PML-mediated viral restriction are sequential. To test this possibility, HSV-1 replication was evaluated in cells co-depleted for PML and PIAS1 (Fig. 7A and B). In the absence of PIAS1 and PML, the PFE of ICP0-null mutant HSV-1 was twice that in cells depleted of either protein alone (Fig. 7C). This data suggests that the antiviral mechanisms of PIAS1 and PML are likely additive. Under conditions in which PIAS1 and PML were co-depleted, the replication of wild-type HSV-1 was not substantially affected, confirming that neither protein is essential for viral replication and that ICP0 is sufficient to counteract their intrinsic antiviral activities (Fig. 7C).

The intrinsic antiviral mechanisms of PIAS1 and PIAS4 are cooperative.

The identification of PIAS1 as an intrinsic antiviral PML-NB constituent protein complements the recent identification of PIAS4 as an intrinsic antiviral factor (30). As PIAS4 localizes to domains that contain HSV-1 genomes throughout infection (30), whether or not PIAS1 also accumulates in replication compartments was evaluated. During ICP0-null mutant HSV-1 infection, PIAS1 localized to replication compartments, although this localization phenotype was less prominent than that of PIAS4 (Fig. 8A). Moreover, the localization of PIAS1 in HSV-1 replication compartments was disrupted by ICP0 (Fig. 8B), whereas PIAS4 remained associated with replication compartments irrespective of ICP0 expression (Fig. 8B) (30).

To test the functional relationship between the antiviral activities of PIAS1 and PIAS4, HSV-1 replication was evaluated in cells depleted of both proteins. Transgenic HFt cells that expressed PIAS1 or PIAS4 specific shRNA had considerable, although not full, depletion of either protein (Fig. 8C). Single or co-depletion of PIAS1 and PIAS4 did not substantially alter the replication of wild-type HSV-1, confirming that ICP0 is sufficient to counteract their

antiviral activities and that these proteins are not essential for HSV-1 replication (Fig. 8D). Depletion of either PIAS1 or PIAS4 enhanced the replication of ICP0-null mutant HSV-1 to a similar degree, while co-depletion of PIAS1 and PIAS4 enhanced it to an even greater degree than did single depletion alone (Fig. 8D). PIAS1 and PIAS4 therefore likely mediate the restriction of ICP0-null mutant HSV-1 through cooperative but independent mechanisms, suggesting that the complementary functional roles of PIAS proteins in the regulation of innate immunity are mirrored in their regulation of intrinsic immunity.

DISCUSSION

We identify PIAS1 as a PML-NB constituent protein that contributes to the repression of ICP0-null mutant HSV-1 replication mediated by the intrinsic antiviral immune response. PIAS1 associates with PML-NBs through SIM-dependent mechanisms that require SUMOylation competent PML and is recruited to nuclear domains that contain infecting HSV-1 genomes through SIM-dependent mechanisms that are enhanced by PML. The stable accumulation of SUMO1 at domains that contain infecting HSV-1 genomes is enhanced by PIAS1, while the stable localization of other major PML-NB constituent proteins at these domains is largely independent of PIAS1. The antiviral mechanisms of PIAS1 are additive to those of PML and cooperative with those of PIAS4. However, the antiviral activities of PIAS1 are efficiently counteracted by ICP0, which abrogates the stable accumulation of PIAS1 in nuclear domains that contain viral genomes. Similar to Daxx, the antagonism of PIAS1 occurs without directly targeting it for degradation (32).

475 PIAS1 is unique amongst the PIAS family of SUMO ligases in that it is the only member
476 that substantially associates with PML-NBs in HFt cells (Fig. 1) (30). This localization of
477 PIAS1 was not restricted to HFt cells, however, as it also colocalized with PML-NBs in other
478 restrictive cell types (Fig. 1C). Given that the PIAS family of proteins have highly conserved
479 SIMs (80% amino acid identity), the SIM-mediated association of PIAS1 with PML-NBs is
480 likely contextual rather than due to generic interactions with SUMO moieties. PML.I.4KR
481 aggregates contain SUMO1, and to a much lesser degree SUMO2/3 (Fig. 3D). In this context,
482 SUMO1 is not sufficient to facilitate the stable localization of PIAS1 at the PML.I.4KR
483 aggregates. Even though the SIM (VIDLT) of PIAS1 does not preferentially bind to a particular
484 SUMO isoform (46, 47), peptides that contain the core SIM sequence (I/V)DLT preferentially
485 bind to SUMO2/3 (48). PIAS1 localization at PML-NBs could therefore be largely mediated
486 through SUMO2/3 interactions. Alternatively, but not exclusively so, specific SUMOylated
487 proteins, potentially PML, may regulate PIAS1 localization at PML-NBs. The association of
488 Sp100 with PML-NBs is not mediated by the Sp100 SIM (49), which superficially suggests that
489 Sp100 should localize to the PML.I.4KR aggregates (Fig. 3D). However, the localization of
490 Sp100 at PML-NBs is mediated by MORC3 (50-52), which does associate with PML-NBs
491 through SIM-dependent mechanisms (53). Sp100 association with PML-NBs is thus indirectly
492 mediated through the SIM of MORC3. PIAS1 specific interactions with particular SUMOylated
493 proteins within PML-NBs may therefore provide the specificity for the stable association of
494 PIAS1, but not other PIAS family members, at these structures.
495 The mechanism whereby PIAS1 is recruited to nuclear domains that contain infecting
496 HSV-1 genomes is similar to that of other PML-NB constituent proteins in that it is SIM
497 dependent, but is also unique in that it is enhanced by PML. In the absence of PML, the

498 localization of PIAS1 at the nuclear edge associated with viral genome entry is substantially
499 reduced (Fig. 5A), indicating that PML is required for the efficient or stable accumulation of
500 PIAS1 at these sites. However, PIAS1 and PML do not fully colocalize within these nuclear
501 domains and puncta that primarily contain only PIAS1 or PML are evident (Fig. 4D). These data
502 suggest that PIAS1 can stably remain within domains that contain infecting HSV-1 genomes
503 through interactions that are likely independent of PML, however, such interactions are not
504 sufficient to mediate its stable re-localization in the absence of PML. Although the accumulation
505 of PIAS1 in nuclear domains that contain infecting HSV-1 genomes is largely PML-dependent,
506 the antiviral effects of PIAS1 are additive to those of PML (Fig. 7C), which demonstrates that
507 they have separate antiviral mechanisms. Thus, in the absence of PML, and consequently the
508 stable accumulation of PIAS1 in nuclear domains that contain infecting viral genomes, PIAS1
509 retains antiviral activities. Conversely, the antiviral mechanisms of PML are not exclusively
510 linked to its capacity to recruit PIAS1 to nuclear domains that contain infecting HSV-1 genomes.
511 It has been reported that the accumulation of SUMO1 within nuclear domains that
512 contain infecting HSV-1 genomes represents SUMOylated PML, as conditions that limit the
513 recruitment of PML also decrease the accumulation of SUMO1 at the recruitment edge (10, 21,
514 24). However, we now show that in the absence of PML, the lack of SUMO1 accumulation at
515 the recruitment edge is likely a secondary effect of the inefficient recruitment of PIAS1 (Figs. 5A
516 and 6D). PIAS1 may promote the accumulation of SUMO1 at the recruitment edge through
517 direct SUMOylation of target substrates. However, preferential PIAS1-mediated SUMO1-
518 modification rather than SUMO2/3-modification of target substrates has yet to be demonstrated.
519 Alternatively, PIAS1 could promote the accumulation of SUMO1 at the recruitment edge
520 through interactions with specific SUMO1-modified proteins. It is unlikely, however, that the

521 efficient accumulation of SUMO1 in nuclear domains that contain infecting HSV-1 genomes
522 represents the primary mechanism of PIAS1 antiviral activity. The depletion of PML disrupts
523 PIAS1, and consequently SUMO1, accumulation in nuclear domains that contain infecting HSV-
524 1 genomes. The accumulation of SUMO1 at such domains is therefore impaired in the absence
525 of either PML or PIAS1, whereas the depletion of both proteins impairs the intrinsic immune
526 response to a greater degree than the depletion of either protein alone (Fig. 7C).

527 PIAS1 is the only PIAS protein that substantially associates with PML-NBs in HFt cells
528 (Fig. 1). However, PML-NB formation, PML SUMOylation, or the localization of SUMO-1 or -
529 2/3 within PML-NBs is not obviously altered in PIAS1 depleted cells (Fig. 6). This observation
530 suggests that PIAS1 is largely not responsible for the SUMOylation events that are crucial for
531 PML-NB stabilization, constitutive PML SUMOylation, or the localization of SUMO-1 or -2/3 at
532 PML-NBs. Alternatively, other PIAS family members (or SUMO E3 ligases) may mediate these
533 events under conditions of PIAS1 depletion, or it is possible that the PIAS1 at PML-NBs largely
534 functions to regulate PML turnover (31). However, this later scenario is unlikely as we did not
535 observe any significant accumulation of unmodified PML following the depletion of PIAS1 (Fig.
536 6A). During ICP0-null mutant HSV-1 infection, the depletion of PIAS1 dramatically reduces
537 SUMO1 accumulation at the nuclear edge that contains infecting HSV-1 genomes (Fig. 6D),
538 suggesting that other SUMO E3 ligases do not efficiently mediate this particular PIAS1 function.
539 PIAS1 and PIAS4 are currently the only PIAS proteins identified to be intrinsic antiviral factors
540 (this manuscript, (30)). While both proteins localize to nuclear domains that contain viral DNA
541 throughout infection, PIAS1 is more prominently recruited to domains that contain infecting
542 HSV-1 genomes while PIAS4 is more prominently recruited into replication compartments (Fig.
543 8A and B) (30). The localization phenotypes of PIAS1 and PIAS4 during HSV-1 infection

suggest that they have shared as well as distinct antiviral activities. Consistently, the antiviral mechanisms of PIAS1 and PIAS4 are cooperative (Fig. 8D). Moreover, PIAS1 and PIAS4 both complement the antiviral activities of PML (Fig. 7C) (30). Together, these data indicate that PIAS proteins likely utilize a multi-faceted yet interconnected approach to modulate intrinsic immunity to achieve the ultimate objective of viral repression.

FUNDING INFORMATION

This work was supported by the Medical Research Council (MRC) grant number MC_UU_12014/5 to C.B and G0801822. The funding organizations had no role in the design of the study, collection or interpretation of the data, or the decision to submit the work for publication.

ACKNOWLEDGEMENTS

We thank Hans Will for the anti-Sp100 antibody SpGH and Roger Everett for HSV-1 reagents. We would also like to thank the members of the CB group for their constructive comments throughout this study.

REFERENCES

1. **Yan N, Chen ZJ.** 2012. Intrinsic antiviral immunity. Nat Immunol **13:**214-222.

2. **Everett RD, Boutell C, Hale BG.** 2013. Interplay between viruses and host sumoylation pathways. Nat Rev Microbiol **11:**400-411.

3. **Blanco-Melo D, Venkatesh S, Bieniasz PD.** 2012. Intrinsic cellular defenses against human immunodeficiency viruses. Immunity **37:**399-411.

4. **Everett RD, Chelbi-Alix MK.** 2007. PML and PML nuclear bodies: implications in antiviral defence. Biochimie **89:**819-830.

5. **Jensen K, Shiels C, Freemont PS.** 2001. PML protein isoforms and the RBCC/TRIM motif. Oncogene **20:**7223-7233.

6. **Kamitani T, Kito K, Nguyen HP, Wada H, Fukuda-Kamitani T, Yeh ET.** 1998. Identification of three major sentrinization sites in PML. J Biol Chem **273:**26675-26682.

7. **Ishov AM, Sotnikov AG, Negorev D, Vladimirova OV, Neff N, Kamitani T, Yeh ET, Strauss JF, 3rd, Maul GG.** 1999. PML is critical for ND10 formation and recruits the PML-interacting protein daxx to this nuclear structure when modified by SUMO-1. J Cell Biol **147:**221-234.

8. **Zhong S, Muller S, Ronchetti S, Freemont PS, Dejean A, Pandolfi PP.** 2000. Role of SUMO-1-modified PML in nuclear body formation. Blood **95:**2748-2752.

9. **Cuchet D, Sykes A, Nicolas A, Orr A, Murray J, Sirma H, Heeren J, Bartelt A, Everett RD.** 2011. PML isoforms I and II participate in PML-dependent restriction of HSV-1 replication. J Cell Sci **124:**280-291.

10. **Cuchet-Lourenco D, Boutell C, Lukashchuk V, Grant K, Sykes A, Murray J, Orr A, Everett RD.** 2011. SUMO pathway dependent recruitment of cellular repressors to herpes simplex virus type 1 genomes. PLoS Pathog **7:**e1002123.

11. **Enserink JM.** 2015. Sumo and the cellular stress response. Cell Div **10:**4.

12. **Tatham MH, Jaffray E, Vaughan OA, Desterro JM, Botting CH, Naismith JH, Hay RT.** 2001. Polymeric chains of SUMO-2 and SUMO-3 are conjugated to protein substrates by SAE1/SAE2 and Ubc9. J Biol Chem **276:**35368-35374.

13. **Hay RT.** 2005. SUMO: a history of modification. Mol Cell **18:**1-12.

14. **Gareau JR, Lima CD.** 2010. The SUMO pathway: emerging mechanisms that shape specificity, conjugation and recognition. Nat Rev Mol Cell Biol **11:**861-871.

15. **Palvimo JJ.** 2007. PIAS proteins as regulators of small ubiquitin-related modifier (SUMO) modifications and transcription. Biochem Soc Trans **35:**1405-1408.

16. **Rytinki MM, Kaikkonen S, Pehkonen P, Jaaskelainen T, Palvimo JJ.** 2009. PIAS proteins: pleiotropic interactors associated with SUMO. Cell Mol Life Sci **66:**3029-3041.

17. **Wimmer P, Schreiner S, Dobner T.** 2012. Human pathogens and the host cell SUMOylation system. J Virol **86:**642-654.

18. **Varadaraj A, Mattoscio D, Chiocca S.** 2014. SUMO Ubc9 enzyme as a viral target. IUBMB Life **66:**27-33.

19. **Maul GG, Ishov AM, Everett RD.** 1996. Nuclear domain 10 as preexisting potential replication start sites of herpes simplex virus type-1. Virology **217:**67-75.

20. **Everett RD, Murray J.** 2005. ND10 components relocate to sites associated with herpes simplex virus type 1 nucleoprotein complexes during virus infection. J Virol **79:**5078-5089.

21. **Boutell C, Cuchet-Lourenco D, Vanni E, Orr A, Glass M, McFarlane S, Everett RD.** 2011. A viral ubiquitin ligase has substrate preferential SUMO targeted ubiquitin ligase activity that counteracts intrinsic antiviral defence. PLoS Pathog **7:**e1002245.

22. **Everett RD, Rechter S, Papior P, Tavalai N, Stamminger T, Orr A.** 2006. PML contributes to a cellular mechanism of repression of herpes simplex virus type 1 infection that is inactivated by ICP0. J Virol **80:**7995-8005.

23. **Everett RD, Parada C, Gripon P, Sirma H, Orr A.** 2008. Replication of ICP0-null mutant herpes simplex virus type 1 is restricted by both PML and Sp100. J Virol **82:**2661-2672.

24. **Glass M, Everett RD.** 2013. Components of promyelocytic leukemia nuclear bodies (ND10) act cooperatively to repress herpesvirus infection. J Virol **87:**2174-2185.

25. **Boutell C, Everett RD.** 2013. Regulation of alphaherpesvirus infections by the ICP0 family of proteins. J Gen Virol **94:**465-481.

26. **Sloan E, Tatham MH, Groslambert M, Glass M, Orr A, Hay RT, Everett RD.** 2015. Analysis of the SUMO2 Proteome during HSV-1 Infection. PLoS Pathog **11:**e1005059.

27. **Stow ND, Stow EC.** 1986. Isolation and characterization of a herpes simplex virus type 1 mutant containing a deletion within the gene encoding the immediate early polypeptide Vmw110. J Gen Virol **67 (Pt 12):**2571-2585.

28. **Everett RD.** 1989. Construction and characterization of herpes simplex virus type 1 mutants with defined lesions in immediate early gene 1. J Gen Virol **70 (Pt 5):**1185-1202.

29. **Everett RD, Boutell C, Orr A.** 2004. Phenotype of a herpes simplex virus type 1 mutant that fails to express immediate-early regulatory protein ICP0. J Virol **78:**1763-1774.

30. **Conn KL, Wasson P, McFarlane S, Tong L, Brown JR, Grant KG, Domingues P, Boutell C.** 2016. A novel role for Protein Inhibitor of Activated STAT 4 (PIAS4) in the

restriction of herpes simplex virus 1 (HSV-1) by the cellular intrinsic antiviral immune response. J Virol doi:10.1128/JVI.03055-15.

31. **Rabellino A, Carter B, Konstantinidou G, Wu SY, Rimessi A, Byers LA, Heymach JV, Girard L, Chiang CM, Teruya-Feldstein J, Scaglioni PP.** 2012. The SUMO E3-ligase PIAS1 regulates the tumor suppressor PML and its oncogenic counterpart PML-RARA. Cancer Res **72:**2275-2284.

32. **Lukashchuk V, Everett RD.** 2010. Regulation of ICP0-null mutant herpes simplex virus type 1 infection by ND10 components ATRX and hDaxx. J Virol **84:**4026-4040.

33. **Smith MC, Goddard ET, Perusina Lanfranca M, Davido DJ.** 2013. hTERT extends the life of human fibroblasts without compromising type I interferon signaling. PLoS One **8:**e58233.

34. **Gripon P, Rumin S, Urban S, Le Seyec J, Glaise D, Cannie I, Guyomard C, Lucas J, Trepo C, Guguen-Guillouzo C.** 2002. Infection of a human hepatoma cell line by hepatitis B virus. Proc Natl Acad Sci U S A **99:**15655-15660.

35. **Everett RD, Sourvinos G, Orr A.** 2003. Recruitment of herpes simplex virus type 1 transcriptional regulatory protein ICP4 into foci juxtaposed to ND10 in live, infected cells. J Virol **77:**3680-3689.

36. **Busnadiego I, Kane M, Rihn SJ, Preugschas HF, Hughes J, Blanco-Melo D, Strouvelle VP, Zang TM, Willett BJ, Boutell C, Bieniasz PD, Wilson SJ.** 2014. Host and viral determinants of Mx2 antiretroviral activity. J Virol **88:**7738-7752.

37. **Sternsdorf T, Guldner HH, Szostecki C, Grotzinger T, Will H.** 1995. Two nuclear dot-associated proteins, PML and Sp100, are often co-autoimmunogenic in patients with primary biliary cirrhosis. Scand J Immunol **42:**257-268.

38. **Everett RD, Cross A, Orr A.** 1993. A truncated form of herpes simplex virus type 1 immediate-early protein Vmw110 is expressed in a cell type dependent manner. Virology **197:**751-756.

39. **Showalter SD, Zweig M, Hampar B.** 1981. Monoclonal antibodies to herpes simplex virus type 1 proteins, including the immediate-early protein ICP 4. Infect Immun **34:**684-692.

40. **Schenk P, Pietschmann S, Gelderblom H, Pauli G, Ludwig H.** 1988. Monoclonal antibodies against herpes simplex virus type 1-infected nuclei defining and localizing the ICP8 protein, 65K DNA-binding protein and polypeptides of the ICP35 family. J Gen Virol **69 (Pt 1):**99-111.

41. **McClelland DA, Aitken JD, Bhella D, McNab D, Mitchell J, Kelly SM, Price NC, Rixon FJ.** 2002. pH reduction as a trigger for dissociation of herpes simplex virus type 1 scaffolds. J Virol **76:**7407-7417.

42. **Lin DY, Huang YS, Jeng JC, Kuo HY, Chang CC, Chao TT, Ho CC, Chen YC, Lin TP, Fang HI, Hung CC, Suen CS, Hwang MJ, Chang KS, Maul GG, Shih HM.** 2006. Role of SUMO-interacting motif in Daxx SUMO modification, subnuclear localization, and repression of sumoylated transcription factors. Mol Cell **24:**341-354.

43. **Shen TH, Lin HK, Scaglioni PP, Yung TM, Pandolfi PP.** 2006. The mechanisms of PML-nuclear body formation. Mol Cell **24:**331-339.

44. **Kahyo T, Nishida T, Yasuda H.** 2001. Involvement of PIAS1 in the sumoylation of tumor suppressor p53. Mol Cell **8:**713-718.

45. **Mostafa HH, Thompson TW, Davido DJ.** 2013. N-terminal phosphorylation sites of herpes simplex virus 1 ICP0 differentially regulate its activities and enhance viral replication. J Virol **87:**2109-2119.

46. **Sun H, Hunter T.** 2012. Poly-small ubiquitin-like modifier (PolySUMO)-binding proteins identified through a string search. J Biol Chem **287:**42071-42083.

47. **Stehmeier P, Muller S.** 2009. Phospho-regulated SUMO interaction modules connect the SUMO system to CK2 signaling. Mol Cell **33:**400-409.

48. **Namanja AT, Li YJ, Su Y, Wong S, Lu J, Colson LT, Wu C, Li SS, Chen Y.** 2012. Insights into high affinity small ubiquitin-like modifier (SUMO) recognition by SUMO-interacting motifs (SIMs) revealed by a combination of NMR and peptide array analysis. J Biol Chem **287:**3231-3240.

49. **Sternsdorf T, Jensen K, Reich B, Will H.** 1999. The nuclear dot protein sp100, characterization of domains necessary for dimerization, subcellular localization, and modification by small ubiquitin-like modifiers. J Biol Chem **274:**12555-12566.

50. **Koken MH, Puvion-Dutilleul F, Guillemin MC, Viron A, Linares-Cruz G, Stuurman N, de Jong L, Szostecki C, Calvo F, Chomienne C, et al.** 1994. The t(15;17) translocation alters a nuclear body in a retinoic acid-reversible fashion. EMBO J **13:**1073-1083.

51. **Sternsdorf T, Jensen K, Zuchner D, Will H.** 1997. Cellular localization, expression, and structure of the nuclear dot protein 52. J Cell Biol **138:**435-448.

52. **Takahashi K, Yoshida N, Murakami N, Kawata K, Ishizaki H, Tanaka-Okamoto M, Miyoshi J, Zinn AR, Shime H, Inoue N.** 2007. Dynamic regulation of p53 subnuclear localization and senescence by MORC3. Mol Biol Cell **18:**1701-1709.

53. **Mimura Y, Takahashi K, Kawata K, Akazawa T, Inoue N.** 2010. Two-step colocalization of MORC3 with PML nuclear bodies. J Cell Sci **123:**2014-2024.

FIGURE LEGENDS

FIG 1. PIAS1 is a PML-NB constituent protein. (A) Confocal microscopy images show the nuclear localization of PIAS1-4 with respect to PML, the major PML-NB scaffolding protein, in HFt cells. The localization of Daxx, a major PML-NB constituent protein, with respect to PML is shown for comparison. PIAS1-4 (red), Daxx (red), and PML (green) were visualised by indirect immunofluorescence. Cut mask (yellow) highlights regions of colocalization; weighted colocalization coefficients are indicated. (B) Box and whisker plot shows the distribution of individual weighted colocalization coefficients of Daxx or PIAS1-4 with PML. The number of nuclei evaluated for each pairwise comparison is shown. Box, upper to lower quartile; diamond, mean; horizontal line, median; upper whisker, maximum value; lower whisker, minimum value. (C) Confocal microscopy images show the nuclear localization of PIAS1 and PML in HFs, HEL, HepaRG, or RPE cells. PIAS1 (red) and PML (green) were visualised by indirect immunofluorescence. Nuclei were stained with DAPI (blue).

FIG 2. Ectopic PIAS1 associates with and disrupts PML-NBs in a SIM- and SUMO ligase-dependent manner. (A) Diagram highlights the PIAS family conserved functional domains (grey) within PIAS1. SAP, SAF-A/B, Acinus and PIAS; PINIT, 'PINIT' motif; SP-RING, Siz/PIAS-RING zinc finger; SIM, SUMO interaction motif; C-Term, variable C-terminal domain. (B-C) Confocal microscopy images show the nuclear localization of eYFP (B) or

eYFP-PIAS1 (C) with respect to PML. EYFP or eYFP-PIAS1 expression was DOX induced (+Dox), or not (-Dox), for 8 or 16 h. PML (red) was visualized by indirect immunofluorescence. (D-E) Emission spectra show the pixel intensity and colocalization between PML and eYFP (D) or eYFP-PIAS1 (E) in the regions indicated by white bars in (B) or (C), respectively. (F) Confocal microscopy images show the nuclear localization of eYFP or catalytically inactive eYFP-PIAS1, with (eYFP.P1.C351A.mSIM) or without (eYFP.P1.C351A) a mutant SIM, with respect to PML-NBs. Expression of eYFP or eYFP-PIAS1 mutant proteins was DOX induced for 16 h. PML-NBs were identified by the accumulation of PML. PIAS1 (pAb; red) and PML (cyan) were visualized by indirect immunofluorescence. Nuclei were stained with DAPI (blue).

FIG 3. PIAS1 localization at PML-NBs requires SUMO-modified PML. (A) Western blots show PML and PIAS1 protein levels in transgenic cells that express PML specific shRNA (shPML) or a non-targeted control sequence (shCtrl). Whole cell lysates were resolved by Tris-glycine SDS-PAGE. Membranes were probed for PML or PIAS1, and actin as a loading control. Molecular weights (MWs) are indicated (kDa). (B) Confocal microscopy images show the nuclear localization of PIAS1 in transgenic HFt cells that express shPML or shCtrl. PIAS1 (red) and PML (green) were detected by indirect immunofluorescence. (C-D) Confocal microscopy images show PIAS1 localization with respect to PML isoform I in PML depleted transgenic HFt cells stably reconstituted with PML.I (eYFP.PML.I; C) or SUMOylation deficient PML.I (eYFP.PML.I.4KR; D). PIAS1 (red), Daxx (red), Sp100 (red), SUMO1 (red), SUMO2/3 (red), and PML (cyan) were detected by indirect immunofluorescence. Nuclei were stained with DAPI (blue).

746 **FIG 4.** ICP0 disperses PIAS1 away from domains that contain infecting HSV-1 genomes
747 without targeting it for proteasomal degradation. (A) Western blots show PIAS1 protein levels
748 during wild-type or ICP0-null mutant HSV-1 infection. HFt cells were infected with 10 PFU of
749 wild-type (HSV-1) or ICP0-null mutant (ΔICP0) HSV-1 per cell in the presence (+) or absence (-
750) of the proteasome inhibitor MG132. Whole cell lysates were harvested at 3, 6, or 9 hours post
751 infection (hpi) and proteins were resolved by Tris-tricine SDS-PAGE. Membranes were probed
752 for PIAS1, PML as an example of an ICP0 substrate, ICP0, ICP4, and UL42 to show the
753 progression of infection, and actin as a loading control. MWs are indicated (kDa). (B) Bar
754 graph shows the average relative levels of PIAS1 during wild-type or ICP0-null mutant HSV-1
755 infection. The intensity of PIAS1 protein bands were quantitated from western blots as in (A),
756 normalised to their respective loading control, and presented as a ratio to the level in mock-
757 infected cells at 9 hpi (1.0). Means and Standard Error of the Means (SEM) are shown (n = 7). *
758 $P < 0.05$, ** $P < 0.01$; Student's two-tailed *t*-test. (C) Confocal microscopy images show the
759 accumulation of PIAS1, or lack of it, at the nuclear edge associated with HSV-1 genome entry in
760 cells within the periphery of a developing plaque (20). HFt cells were infected with 2 or 0.002
761 PFU per cell of ICP0-null mutant or wild type HSV-1, respectively, for 16 h. PIAS1 (red), PML
762 (cyan), and Daxx (cyan) were detected by indirect immunofluorescence. The nuclear edge
763 associated with HSV-1 genome entry was identified by eYFP.ICP4 localization. Nuclei were
764 stained with DAPI (blue). (D) Three-dimensional reconstruction of z-stack series of confocal
765 microscopy images shows the accumulation of PIAS1 and PML at the nuclear edge associated
766 with HSV-1 genome entry. Regions of PML and PIAS1 colocalization (yellow) are highlighted;
767 Pearson coefficient is indicated.
768

FIG 5. The SIM-dependent localization of PIAS1 at domains that contain infecting HSV-1 genomes is enhanced by PML. (A) Confocal microscopy images show PIAS1 localization, or lack of it, at nuclear domains that contain infecting HSV-1 genomes in transgenic PML depleted (shPML) or not (shCtrl) HFt cells within a developing plaque. Cells were infected with 2 PFU of ICP0-null mutant HSV-1 (ΔICP0) per cell for 16 h. PIAS1 (red), PML (cyan), and Daxx (cyan) were detected by indirect immunofluorescence. (B) Confocal microscopy images show the nuclear localization of eYFP or eYFP-PIAS1 mutant proteins in HSV-1 infected cells within a developing plaque. EYFP or eYFP-PIAS1 mutant protein expression was DOX induced for 4 h prior to infection with 2 PFU of ICP0-null mutant HSV-1 (ΔICP0) or 0.002 PFU of wild-type HSV-1 (HSV-1) per cell for 16 h. ICP4 (red) and PML (cyan) were detected by indirect immunofluorescence. The nuclear edge associated with HSV-1 genome entry is identified by ICP4 localization. Nuclei were stained with DAPI (blue). (C) Western blots show the expression level of eYFP-PIAS1 mutant proteins. Protein expression was DOX induced for 0, 8, or 24 h prior to the collection of whole cell lysates. Membranes were probed for PIAS1 and actin as a loading control. MWs are indicated (kDa).

FIG 6. PIAS1 is not essential for PML-NB formation or PML SUMOylation, but does enhance the accumulation of SUMO1 in domains that contain infecting HSV-1 genomes. (A) Western blots show PIAS1 protein levels in transgenic HFt cells that express PIAS1 specific (shPIAS1) or non-targeted control (shCtrl) shRNA. Whole cell lysates were resolved by Tris-glycine SDS-PAGE. Membranes were probed for PIAS1 or PML, and actin as a loading control. MWs are indicated (kDa). (B) Confocal microscopy images show the localization of PML in transgenic shPIAS1 or shCtrl expressing cells. PML (green) and PIAS1 (red) were detected by indirect

immunofluorescence. (C) Confocal microscopy images show the localization of Daxx, SUMO1, or SUMO2/3 in mock infected HFt cells that express shPIAS1 or shCtrl. Daxx (green), PIAS1 (red), SUMO1 (cyan), and SUMO2/3 (cyan) were detected by indirect immunofluorescence. (D) Confocal microscopy images show the nuclear localization of PML, Daxx, SUMO1, or SUMO2/3 during ICP0-null mutant HSV-1 infection of transgenic HFt cells that express shPIAS1 or shCtrl. Cells were infected with 2 PFU of ICP0-null mutant HSV-1 per cell for 16 h. PIAS1 (red), PML (cyan), Daxx (cyan), SUMO1 (cyan), and SUMO2/3 (cyan) were detected by indirect immunofluorescence. The nuclear edge associated with HSV-1 genome entry was identified by eYFP.ICP4 localization. Nuclei were stained with DAPI (blue).

FIG 7. PIAS1 repression of ICP0-null mutant HSV-1 replication is additive to that of PML. (A) Bar graph shows the average relative levels of PML or PIAS1 mRNA in transgenic HFt cells that express shRNA against PML (shPML), PIAS1 (shPIAS1), or a non-targeted control (shCtrl). PML or PIAS1 mRNA levels were determined using the TaqMan system of quantitative RT-PCR. Values normalized to GAPDH expression using the ΔΔCt method are expressed relative to mock-infected cells (1.0). Means and Standard Deviations (SD) are shown ($n > 3$). (B) Western blots show PML or PIAS1 protein levels in transgenic HFt cells that express shPML, shPIAS1, or shCtrl. Whole cell lysates were resolved by Tris-glycine SDS-PAGE. Membranes were probed for PML or PIAS1, and actin as a loading control. MWs are indicated (kDa). (C) Bar graph shows the average relative plaque forming efficiency (PFE) of wild-type (HSV-1) or ICP0-null mutant (ΔICP0) HSV-1 in transgenic HFt cells that express shCtrl, shPML, or shPIAS1. The number of plaques for each strain is expressed relative to the corresponding

number of plaques for that strain in shCtrl expressing cells. Means and SD are shown (n = 6). Neo, neomycin; Puro, puromycin.

FIG 8. PIAS1 and PIAS4 cooperatively restrict ICP0-null mutant HSV-1 replication. (A-B) Confocal microscopy images show the localization of PIAS1 and PIAS4 in HSV-1 infected cells. HFt cells were infected with 2 or 0.002 PFU per cell of ICP0-null mutant (A) or wild type HSV-1 (B), respectively, for 16 h. PIAS1 (red), PIAS4 (red), and PML (cyan) were visualized by indirect immunofluorescence. Replication compartments were identified by the accumulation of eYFP.ICP4. Insert (dashed box in (A)) highlights a region where PIAS1 and PML colocalize within a replication compartment. Nuclei were stained with DAPI (blue). (C) Western blots show PIAS1 or PIAS4 protein levels in transgenic HFt cells that express shRNA against PIAS1 (shPIAS1), PIAS4 (shPIAS4), or a non-targeted control (shCtrl). Whole cell lysates were resolved by Tris-glycine SDS-PAGE. Membranes were probed for PIAS1 or PIAS4, and actin as a loading control. MWs are indicated (kDa). Puro, puromycin. (D) Bar graph shows the average relative PFE of wild-type or ICP0-null mutant HSV-1 in transgenic HFt cells that express shPIAS1, shPIAS4, or shCtrl. The number of plaques for each strain is expressed relative to the corresponding number of plaques for that strain in cells that express shCtrl. Means and SD are shown (n = 6).

832 **TABLE 1:** Primers for PIAS1 PCR mutagenesis and their corresponding substitution mutations.

833

PIAS1 Mutant	PCR Primers for Mutagenesis		Amino Acid Change
	Forward	Reverse	
C351A	5'GGGCCCTTACAGCGTCTCATCTAC	5'GTAGATGAGACGCTGTAAGGGCCC	C to A
mSIM	5'GAAAGTAGAAGCGGCTGACCTAACCATAG	5'CTATGGTTAGGTCAGCCGCTTCTACTTTC	VIDLT to AADLT

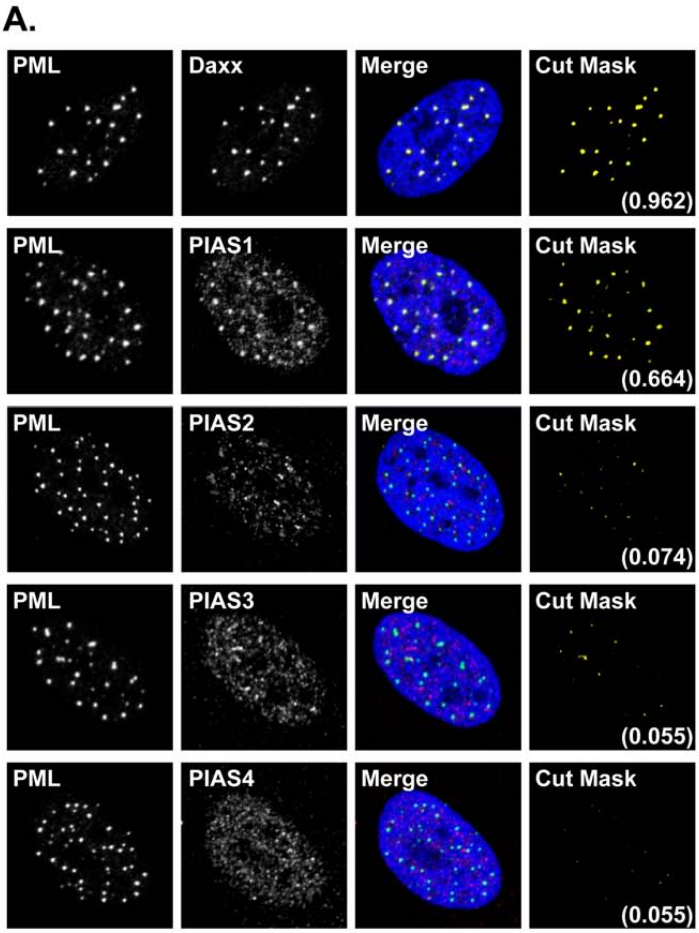

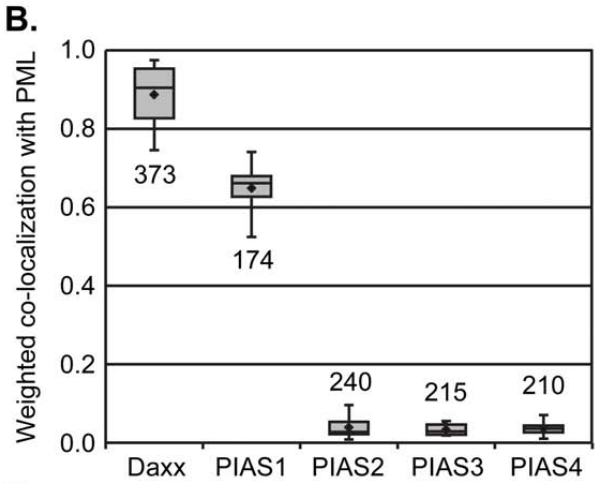

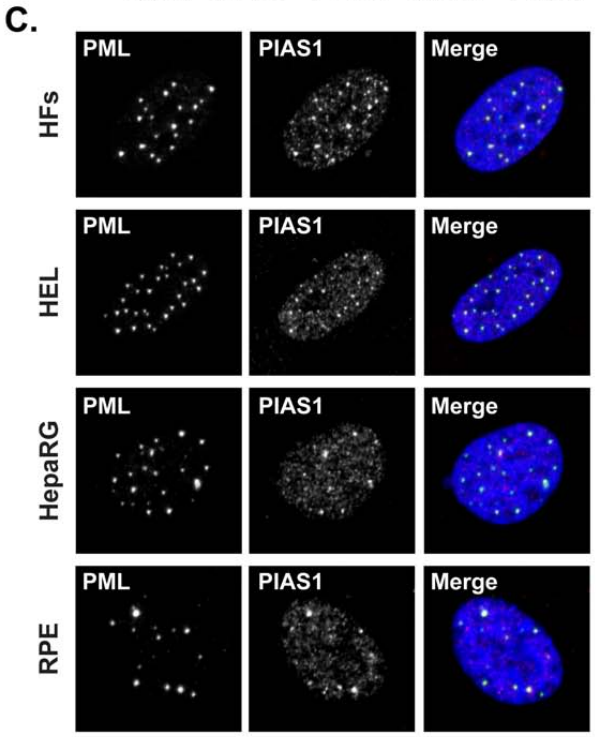

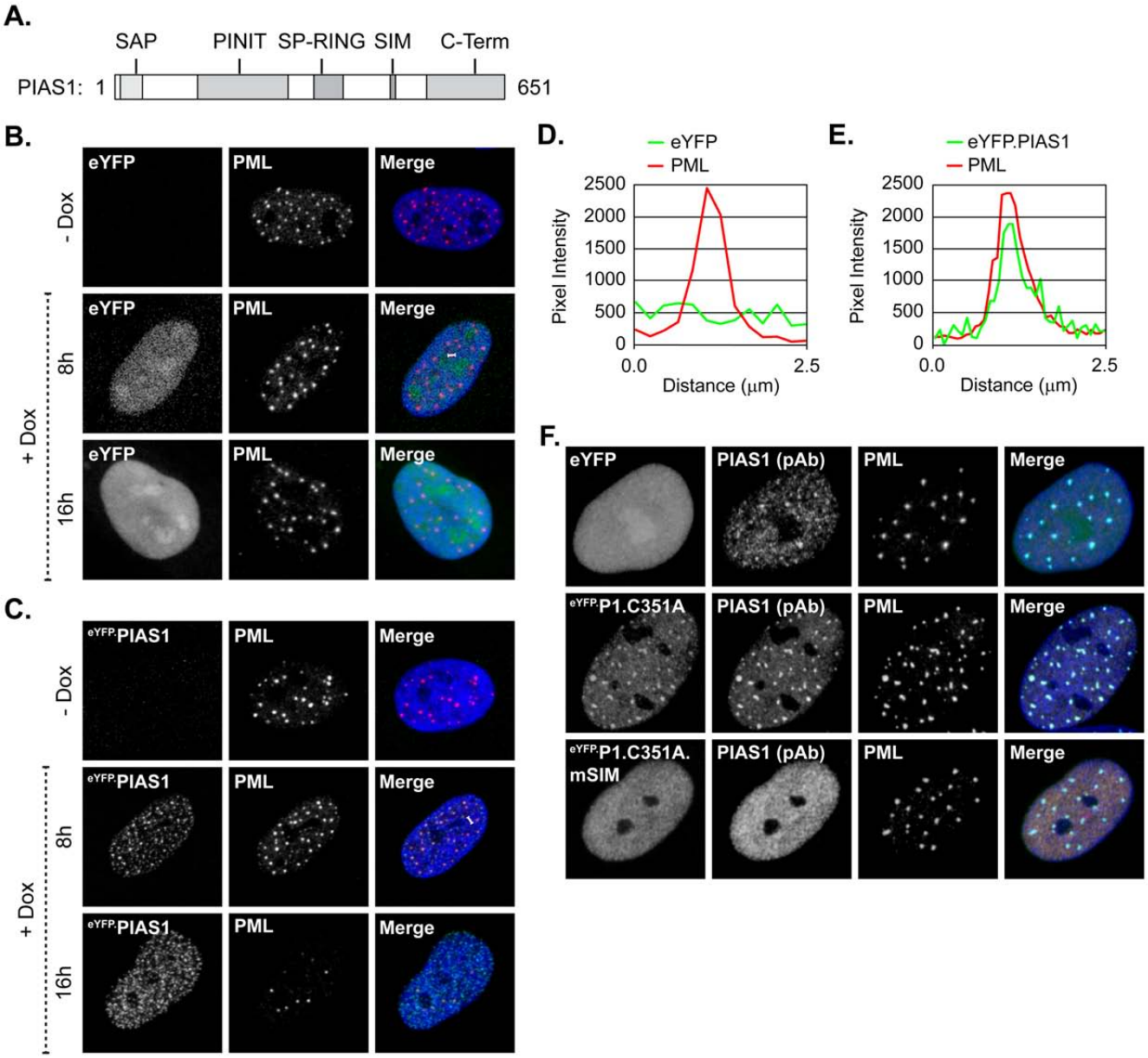

Journal of Virology